Orbital Dynamics in a Stochastic Atmosphere

J. de Lafontaine*
European Space Research and Technology Centre, Noordwijk, the Netherlands

An algorithm is developed to analyze the orbital dynamics of a near-Earth satellite subjected to the random perturbations of a stochastic atmosphere. The orbital equations include the perturbation caused by an oblate geopotential and a drag model where the atmospheric density varies exponentially with height and temporally with the solar-activity and semiannual cycles. A random process representative of short-term density fluctuations modulates this deterministic density function. The solution begins with the analytical averaging of both the gravity and the drag perturbations, following the principle of the Method of Averaging. The drag averages are expanded in a series of newly defined functions called the "two-dimensional hyperbolic Bessel functions." Their nice analytical properties greatly simplify the next part of the solution where the equations of motion are further transformed into a "stochastic Taylor expansion." Unlike the standard linear approach used in the treatment of stochastic systems, this technique preserves the full nonlinearity of the equations of deterministic motion and, therefore, avoids the usual restriction to small excursions from an initial or reference state. The analytical nature of the drag averages provides insight into the orbital effects of random density fluctuations and results in an efficient algorithm that prescribes the evolution of the mean and variance of the orbital state. Based on this algorithm, a computer program has been developed to generate confidence intervals that bound, in a probabilistic sense, the trajectory of a satellite. Typical numerical results assuming a 300-km-high near-circular orbit are illustrated. Although orbital error analysis is the main application of the paper, its analytical results can also be used in the development of an orbit determination and density estimation algorithm.

Introduction

THE analysis and simulation of low-Earth orbit (LEO) dynamics must include in its formulation the dominant influence of the atmospheric drag perturbation. Despite the sophistication of some models, it is well known that the accuracy of LEO predictions is always limited by the unpredictable nature of this perturbation. The long-term fluctuations in density are closely correlated to the 11-yr cycle of the sun and are, therefore, roughly predictable.[1,2] On the other hand, the shorter-term day-to-day variations are unpredictable and, although their impact on the trajectory can be quite determinant, their random nature makes their inclusion in a prediction software a rather complex task. In fact, most of the orbital theories ignore these random inputs in the problem formulation and simply provide comments on the expected uncertainty in their deterministic results. For instance, it has often been observed[3-6] that atmospheric density models cannot have a better accuracy than about $\pm 10\%$. This inaccuracy in the model is directly translated in a proportional uncertainty in position and orbital lifetime.[7]

A more quantitative method of determining the trajectory dispersion caused by uncertainties in solar activity is to propagate the orbit using the 2.3 and 97.7% predictions in solar activity,[8-10] as provided by the NASA Marshall Space Flight Center. Although these data provide a 95% confidence interval in solar activity indices, the same cannot be said of the corresponding trajectory confidence intervals because of the complex and nonlinear relationship between solar activity and satellite trajectory dynamics. Therefore, although this approach gives an indication of the worst-case satellite trajectories, it does not provide statistical information (e.g., expected mean trajectory, standard deviation) on the dynamics and magnitude of the random orbital dispersion. Furthermore, the NASA predictions correspond to 13-month averages of the solar flux index ($\bar{F}_{10.7}$) and do not account for the unpredictable daily variations about its mean ($F_{10.7}-\bar{F}_{10.7}$).

The few truly stochastic algorithms (e.g., Refs. 11 and 12) rely on a linearized version of the equations of motion since, in this case, it is possible to obtain a relatively simple solution to the equations describing the evolution of the state mean and variance. This technique essentially provides an "exact" solution to a simplified set of equations with the consequence of not being valid over large intervals of time. In fact, linearization is normally intended to the analysis of the small displacements of a dynamical system from an equilibrium position. In the present application, no equilibrium exists because of the secular orbital changes induced by the nonconservative drag perturbations.

The objective of this paper is the development of an orbital prediction algorithm that preserves the *full nonlinearity* of the original dynamical equations, but still provides quantitative statistical information on the evolution of a near-Earth orbit subjected to random perturbations. The particularity of the present approach is the application of a stochastic Taylor expansion, which is fairly well known in the literature on probability and statistics,[13] but has never been applied to orbital mechanics problems. The application of this transformation is made possible by the "creation" of a new set of analytic functions called the two-dimensional hyperbolic Bessel functions.[7] The algorithm has been implemented in a computer program that not only predicts the expected trajectory of the satellite but also propagates the variance of the state from this mean. This software is also useful as a tool for sensitivity analyses, orbit determination, and atmospheric density estimation.

The paper also contributes to the fields of atmospheric density modeling and analytical averaging of the drag perturbation. For this reason, details on the mathematical formulation of the problem and on the density model specifically developed for this application will be provided throughout the paper. Finally, a demonstration of the simulation software will illustrate the effects of realistic random density variations on the orbital elements of a 300-km-high, near-circular orbit.

Received Sept. 28, 1987; revision received Dec. 6, 1988.

*Aerospace Engineer. Member AIAA.

Perturbation Model

The analysis of low-orbit dynamics requires as a minimum the modeling of the perturbations caused by air drag and geopotential oblateness.[7,10] In this study devoted to random perturbations, the second effect could be neglected because of its deterministic nature. However, it is nevertheless kept in the formulation, not only because its inclusion will allow more realistic simulations, but also because of its "indirect" random contribution to the orbital state, as will be explained.

Drag Model

In a free molecular flow, the drag specific force acting on a satellite of projected area A, drag coefficient C_D, and mass m can be accurately represented by

$$f = -\frac{1}{2}\rho\frac{C_D A}{m} v_R v_R \tag{1}$$

The determination of the ballistic parameters C_D and A is discussed in Refs. 3, 7, and 14. These references also present the mathematical formulation of the relative velocity vector v_R as a function of the west-to-east rotation of the atmosphere. Here, we will assume a stationary atmosphere and a constant ballistic coefficient in order to concentrate our attention on the source of the random perturbations, the atmospheric density ρ.

The deterministic component of the density model, denoted ρ_D, varies exponentially with altitude z, and its temporal dependence includes the effects of the semiannual and solar-activity cycles.[7,15] The first effect has a relatively large magnitude at low altitude and its period, comparable to that of most orbital lifetime predictions, makes it an important refinement to the model.[4] The second effect accounts for the time variation of the density with the mean solar flux index $\bar{F}_{10.7}$.

The model for the density ρ_D is based on the concept of *local* and *global* models.[7,16] A so-called local exponential model (LEM) represents the density profile along the osculating orbit, and a more complex global exponential model (GEM) periodically calibrates this local version as the orbit progresses and the atmospheric conditions vary. The GEM is an exponential approximation to the Jacchia 1977 standard density model,[15] and its mathematical structure is detailed in Ref. 7. More attention is devoted here to the LEM since, unlike the GEM, it directly enters the formulation of the motion equations.

The altitude and time dependences of the LEM are modeled as

$$\rho_D = \rho_p \exp[\sigma(\gamma - \gamma_p)] \tag{2}$$

where subscript p denotes evaluation at a reference point on the orbit: perigee for a noncircular orbit, ascending node for a circular nonequatorial orbit, and First Point of Aries for a circular-equatorial one.[7] The reciprocal radial distance γ represents the altitude dependence through

$$\gamma \triangleq \frac{1}{r} = (z + r_E)^{-1}, \qquad r_E = \text{Earth radius} \tag{3}$$

The scale-height parameter σ accounts for the large density variations along an eccentric orbit. The particularity of this otherwise conventional model is the fact that σ varies with height:

$$\sigma = \sigma_0 + \sigma_1(\gamma - \gamma_p) \tag{4}$$

In fact, because of analytical difficulties to be described later, the orbital theories using an exponential model[3,4,17-20] have never introduced such a variation *within* the argument of the exponential function and have adopted either a *constant* scale-height parameter, i.e., $\sigma_1 = 0$, or a less powerful correction factor outside the exponential argument. For a better representation of the density variation, it is recognized that the scale height must be a function of altitude.[3,7,21] As a result, empirical formulations based on a power law have often been preferred. In the present paper, a new mathematical development has made possible the use of the more powerful exponential formulation with a variable scale height in its argument. The analytical details of this new approach will be examined later in the paper.

The free parameters ρ_p, σ_0, and σ_1 are regularly updated by the GEM such that the deviation of the local model from the global reference is minimized at all times. The computation of the three free parameters proceeds as follows. First, they are expressed as analytical functions of three "collocation points," where the LEM and the GEM will be made to coincide. Next, by choosing three collocation points on the orbit that minimize the maximum deviation of the LEM from the GEM, the three parameters can be numerically evaluated. Reference 7 investigates the fit of the LEM to the GEM and shows that collocation at perigee (0 deg), apogee (180 deg), and 20 deg from perigee insures the minimization of the maximum differences for most orbital conditions. By including the "symmetric" density variations—like solar activity ($\sim \bar{F}_{10.7}$) and semiannual cycle—in the GEM, these effects become implicitly included in the LEM through the adjustable parameters. Modifications to the above local model to include the "nonsymmetric" density variations (e.g., atmospheric flattening, diurnal bulge, geomagnetic and seasonal-latitudinal cycles) are discussed in Ref. 7, but fall outside the scope of this paper. The updating frequency of the LEM parameters depends on the characteristic time of density variations (with respect to the orbit). Updating at every integration step has been implemented in the simulations presented at the end of this paper.

When we substitute the orbital equation

$$\gamma = \kappa(1 + e\cos\theta) \tag{5}$$

(κ = reciprocal of semilatus rectum, e = orbital eccentricity, θ = true anomaly) and Eq. (4) into Eq. (2), we can rewrite the deterministic density model in a more compact form:

$$\rho_D = \rho_p \exp(x_0 + x_1\cos\theta + x_2\cos^2\theta) \tag{6}$$

with the definitions

$$\left.\begin{aligned} x_0 &\triangleq x(\sigma_1 x - \sigma_0) \\ x_1 &\triangleq x(\sigma_0 - 2\sigma_1 x) \\ x_2 &\triangleq x^2\sigma_1 \end{aligned}\right\} \qquad \text{and} \qquad x = \kappa e \tag{7}$$

Expressions similar to Eq. (6) also exist for the degenerate orbits.[7]

For the stochastic component of the model, the general form developed by Elyasberg and Kugaenko[11] has been adopted here:

$$\rho = \rho_D\left[1 + M(z,t)\Gamma(t)\right] \tag{8}$$

where ρ is the stochastic density, ρ_D the deterministic density of Eq. (6), $M(z,t)$ the modulation factor, and Γ represents the short-term random density variations caused by either the solar activity or the geomagnetic activity. The modulation factor accounts for the variation in the statistical properties of the density with altitude (z) and the phase in the solar cycle (t). It can be verified in Ref. 11 that the altitude dependence can be isolated as

$$M(z,t) = M_1(t)z + M_0(t), \qquad z \geq 90 \text{ km} \tag{9}$$

Although the solution proposed in this paper can accommodate the preceding expression, the modulation factor is further

simplified here by taking its value at the reference point on the orbit, the perigee:

$$M_p = M(z_p, t_p) = M_1(t_p) z_p + M_0(t_p) \tag{10}$$

This simplification is justified by the dominance of air drag at that point.

The second-order statistics of the random process Γ are completely defined by its expected value μ_Γ and its autocorrelation function $C_\Gamma(\tau)$. Reference 11 proposes the following model:

$$\mu_\Gamma \triangleq \mathcal{E}\left[\Gamma(t)\right] = 0 \tag{11}$$

$$C_\Gamma(\tau) \triangleq \mathcal{E}\left[\Gamma(t)\Gamma(t+\tau)\right] = \sigma_\Gamma^2 \exp(-\beta|\tau|) \tag{12}$$

where $\mathcal{E}$ is the expectation operator, and σ^2 denotes the variance. The statistical parameters σ_Γ and β can be chosen to simulate the solar activity contribution $(F_{10.7} - \bar{F}_{10.7})$, or that of the geomagnetic activity $(A_p - \bar{A}_p)$ or $(K_p - \bar{K}_p)$.

Geopotential Model

The major contribution of the gravity perturbation (oblateness) is contained in the second spherical harmonic (J_2) of the geopotential function. Because of its deterministic nature, it will not have a *direct* random contribution to the orbital state. However, its dependence on the satellite position, which is made random by the direct contribution of the density model, will indirectly make the gravitational acceleration random as well. Because it offers the possibility to observe this *indirect* random effect on the state, this conservative perturbation is included in the formulation. The perturbing potential thus takes the form

$$\Phi(r,\phi) = J_2 \frac{GM}{r}\left(\frac{r_{Ee}}{r}\right)^2 P_2(\sin\phi) \tag{13}$$

where ϕ is the satellite latitude, GM the Earth gravitational parameter, and P_2 the Legendre polynomial of order 2.

Solution: Deterministic System

Semianalytic Approach

We begin the development of the equations of motion by neglecting, for the moment, the random factor $\Gamma(t)$. The satellite motion is first expressed as a set of variation-of-parameters (VOP) equations formulated in their Gaussian form. To obtain a fast propagation of the state, the short-period oscillations appearing in the deterministic equations are removed, following the well-known principles of the method of averaging (MOA).[22,23] The recovery of these high-frequency terms can be easily carried out when the osculating orbital state of the satellite is desired. This task is not considered here and, throughout this paper, only the evolution of the averaged orbital elements is discussed. (Hence, unless specified otherwise, "mean trajectory" will refer to statistical average and not to orbital average.) The application of this semianalytic transformation is well documented in Refs. 24–28, and is not repeated here. In its simplest form, it involves the analytical or numerical averaging of the VOP equations over one orbit, so that the integration of the smoothed equations can be carried out with a larger step size.

We shall soon see in the next section that the particular technique adopted for the solution of the stochastic system imposes a severe constraint on the averaging procedure of the deterministic equations: the averages must be obtained in an analytical form. The analytical averaging of the gravitational perturbation is straightforward,[29,30] that of atmospheric drag is not.[31] For this reason, an overview of the drag-averaging procedure is now presented.

Drag Averages

After application of the MOA, it can be shown[7] that, for all the orbital elements, the drag averages involve integrals of the following general form:

$$A(x_0,x_1,x_2) = \frac{1}{2\pi}\int_0^{2\pi} \exp(x_0 + x_1\cos\theta + x_2\cos^2\theta)\left\{\frac{1}{2}\hat{X}_0 + \sum_{n=1}^{\mathcal{L}}\left[\hat{X}_n\cos n\theta + \tilde{X}_n \sin n\theta\right]\right\} d\theta \tag{14}$$

The exponential factor accounts for the altitude variation of the density. We recall from Eqs. (6) and (7) that its arguments x_0, x_1, and x_2 are functions of the density parameters σ_0 (scale height) and σ_1 (scale-height gradient). The Fourier series in the brackets represents the expansion of the so-called "kinematic functions"[7,16] in powers of eccentricity and accounts for the radial distance and velocity of the spacecraft on its orbit. Recurrence relations generating its coefficients $\hat{X}_n$ and $\tilde{X}_n$ have been derived and are documented in Refs. 7 and 16. The series limit $\mathcal{L}$ is automatically adjusted to the orbital eccentricity e, so that a user-chosen tolerance ϵ (e.g., 10^{-15}) can be achieved in the accuracy of the series expansion. The closed-form relation between the series limit $\mathcal{L}$, the eccentricity e, and the tolerance ϵ is also described in the preceding references.

For nonconservative perturbations such as air drag, integrals like Eq. (14) are normally solved using numerical quadratures.[26,31] For reasons that will soon become evident, the current development requires an analytical solution.

In all previous studies, the presence of the scale-height-gradient coefficient x_2 precluded the analytical solution of integral (14). The gradient was either neglected ($x_2 = 0$), despite its importance, or first-order approximations of the form

$$\exp(x_0 + x_1\cos\theta + x_2\cos^2\theta) \simeq \exp(x_0 + x_1\cos\theta)[1 + x_2\cos^2\theta]$$

had to be assumed. In the present paper, the general problem ($x_2 \neq 0$) is solved. To better appreciate the development of the new solution, let us first review the approach taken by the previous theories in which $x_2 = 0$.

For the particular case where $x_2 = 0$, corresponding to a constant-scale-height density model, the integral can be solved in terms of the hyperbolic Bessel functions of order n:

$$A(x_0,x_1,0) = \exp(x_1)\left\{\frac{1}{2}\hat{X}_0 I_0(x_0) + \sum_{n=1}^{\mathcal{L}}\left[\hat{X}_n I_n(x_1)\right]\right\} \tag{15}$$

The well-known functions $I_n(x_1)$ can be evaluated by series expansions and recurrence relations. This analytical approach has been often used in the literature, and the resulting solution is found in all the orbital theories using a constant-scale-height exponential model, for instance Refs. 3, 4, 17–20, and 32. Note that solution (15) is not in closed form because of the infinite series defining the $I_n(x_1)$, but it is nevertheless analytic because it can be evaluated and analyzed using the well-known properties of the Bessel functions.

Using mathematical induction, the author has extended the preceding result to the more general case of Eq. (14) and "created" a new set of functions, denoted by L_n and called the two-dimensional hyperbolic Bessel functions, such that an analytic solution to Eq. (14) now exists. The general solution has the form

$$A(x_0,x_1,x_2) = \exp(x_0)\left\{\frac{1}{2}\hat{X}_0 L_0(x_1,x_2) + \sum_{n=1}^{\mathcal{L}}\left[\hat{X}_n L_n(x_1,x_2)\right]\right\} \tag{16}$$

Similarly to the I_n, the new functions L_n are defined by infinite series:

$$L_n(x_1,x_2) = \frac{1}{2}\sum_{k=n}^{\infty}\lambda_k(x_1,x_2)\alpha_{k,n}$$

with

$$\lambda_k(x_1,x_2)=\sum_{\ell=0,2}^{k}\frac{x_1^{k-\ell}}{(k-\ell)!}\frac{x_2^{\ell/2}}{(\ell/2)!}$$

For computer evaluation, the infinite summation is limited to the number of terms that give the required accuracy. The summation defining the λ_k takes place over even ℓ only, and the $\alpha_{k,n}$ are constants. Recurrence relations and various other properties of the L_n functions have been derived and are documented in Ref. 7. From these properties, it is easy to prove the evident requirement that Eq. (16) must degenerate to Eq. (15) when $x_2=0$, i.e.,

$$L_n(x_1,0)\equiv I_n(x_1) \tag{17}$$

Another nice property of these functions to be exploited in the stochastic solution is the simplicity of their partial derivatives with respect to x_1 and x_2:

$$\frac{\partial L_n(x_1,x_2)}{\partial x_1}=\frac{1}{2}(L_{n+1}+L_{n-1}) \tag{18a}$$

$$\frac{\partial L_n(x_1,x_2)}{\partial x_2}=\frac{1}{4}(L_{n+2}+2L_n+L_{n-2}) \tag{18b}$$

Averaged Equations

The general form of the gravity and drag orbital averages (taken from Ref. 7) is shown in the Appendix, with the orbit number N as the independent variable and time as a dependent variable. It can be observed that drag affects the semimajor axis a and eccentricity e, whereas gravity governs the evolution of the argument of perigee ω, right ascension of ascending node Ω, and time t. Under the present assumptions, the orbital inclination i remains constant. Similar equations for the degenerate cases (circular, equatorial orbits) have also been derived and appear in Ref. 7. When the eccentricity e falls below a user-chosen tolerance, the software switches over to the appropriate set (circular orbits) of equations. Since drag tends to keep the orbit circular, the propagation proceeds assuming $e=0$. This "fixed-singularity" approach[7,9] is a simple alternative to the more accurate use of nonsingular elements (e.g., Ref. 33). It is noted, however, that the stochastic equations developed in this paper can be applied to any set of orbital parameters.

Discretization

Keeping the orbit number as the independent variable, the motion equations are discretized with a sampling interval of one orbital period. The validity and usefulness of this transformation can be summarized as follows:

1) The characteristic time variation in the state caused by the deterministic rate functions is much larger than one orbital period (except at very low altitude, near re-entry, where the drag perturbation becomes of the order of gravity itself. In this case, orbital end-of-life is imminent).

2) The characteristic time variation in the random component of the density (correlation time constant $1/\beta$ of about 6 days according to Ref. 11) is also much larger than one orbital period.

3) Physically, the dominance of atmospheric drag at the perigee of an eccentric orbit causes discrete, staircase-like changes in the orbital elements at every period.[7,16]

4) Analytically, because of point 1 above, the orbital averages are practically identical to a normalized integration of the *perturbed* motion over one orbit.[7] Thus, the MOA effectively provides the per-orbit changes in the orbital elements.

5) Numerically, discretization is inevitable when simulation on a digital computer is contemplated.

6) The use of multiorbit propagation algorithms can significantly increase the efficiency of state propagation.

In matrix form, the discretized equations of motion can be written as

$$\xi_{N+1}=\xi_N+R(\xi_N)+D(\xi_N)\Gamma_N \tag{19}$$

where ξ is the 5×1 column matrix of the orbital variables (remember that i is constant and, therefore, not propagated). The column matrix $R(\xi_N)$ includes the deterministic rates caused by drag and gravity, while $D(\xi_N)$ contains the rates caused by drag multiplied by the modulation factor M_p of Eq. (10). In Eq. (19), the direct random contribution comes from Γ_N and the indirect one from the dependence of the rate functions $R(\xi_N)$, $D(\xi_N)$ on the random state ξ_N.

The correlated sequence Γ_N gives the random component of density at the perigee of the Nth orbit and is generated from an uncorrelated sequence W_N through a linear discrete filter:

$$\Gamma_{N+1}=a\Gamma_N+bW_N \tag{20}$$

The correlation function of W_N is given by

$$C_W=\mathcal{E}\{W_NW_M\}=\delta_{NM}$$

where δ_{NM} is the Kronecker delta.

For a stationary distribution, the statistics of Γ_N must satisfy

$$\mu_{\Gamma N}=\mu_\Gamma=0 \tag{21a}$$

$$\sigma^2_{\Gamma N}=\sigma^2_\Gamma=b^2/(1-a^2) \tag{21b}$$

with a and b constants to be determined. The correlation function for Γ_N is easily shown to be

$$C_\Gamma(K)\triangleq\mathcal{E}\{\Gamma_N\Gamma_{N+K}\}=\sigma^2_\Gamma a^{|K|} \tag{22}$$

By comparing Eq. (22) with Eq. (12), the design equation for a can be derived:

$$a=\left[\frac{C_\Gamma(K)}{\sigma^2_\Gamma}\right]^{1/|K|}=\exp(-\beta\,|\tau/K|) \tag{23}$$

Using Eq. (21b), it is easy to solve for b as well:

$$b=(1-a^2)^{1/2}\sigma_\Gamma \tag{24}$$

Given the second-order properties of the random density distribution function, i.e., σ_Γ and C_Γ (or β), and the fact that for near-Earth satellites $K/\tau\simeq 16$ orbits/day, it is, therefore, possible to solve for the filter parameters a and b.

Solution: Stochastic System

Background

The rates $R(\xi_N)$ and $D(\xi_N)$ are nonlinear functions of the random state vector ξ_N. The complexity introduced by this nonlinear dependence is often avoided by simply neglecting the indirect random contribution from these functions and considering only the direct one from Γ_N. This approach was effectively taken in Ref. 11. A more realistic approach is the linearization of these functions with respect to a deterministic initial or reference state ξ_0, as is done in Ref. 12, thereby taking into account, to first-order, the indirect random contribution. However, this approximation in the rate functions is justified only when the propagation of the state is restricted to small displacements from the initial or reference deterministic state ξ_0. For LEO predictions and orbital lifetime analyses, this restriction is not practical because of the secular effects of drag. Linearization with respect to a reference state is, therefore, of limited use in the present application. Reference 7 presents and discusses a total of four different sets of linearized equations and concludes that, if an approximation has to be used, it should only affect the stochastic component of the solution and not the original deterministic equations.

Thus, the best approach consists in the linearization of the rate functions about the current mean μ_N. In this way, only the random excursions

$$\delta_N \triangleq \xi_N - \mu_N \tag{25}$$

from the mean—and not the full state differences $(\xi_N - \xi_0)$—have to be kept small. For a better accuracy in representing the indirect random contribution, one could extend the preceding principle to a higher order. A stochastic Taylor expansion results.

Stochastic Taylor Expansion

In this paper, a second-order Taylor expansion of the rate functions about the mean state is developed:

$$R(\xi_N) \simeq R_N + \Delta R_N \delta_N + \Delta^2 R_N \delta_N \delta_N^T \tag{26}$$

where

$\delta_N =$ random excursions from the mean, see Eq. (25)

$R_N =$ column matrix of rate functions evaluated at the mean μ_N

$\Delta R_N =$ Jacobian matrix (first-order partial derivatives)

$\Delta^2 R_N =$ Hessian matrix (second-order partial derivatives)

A similar expression exists for $D(\xi_N)$. Notice that the rate functions $R_N = R(\mu_N)$ and $D_N = D(\mu_N)$ still have their original *nonlinear* dependence on the mean state μ_N. The deterministic state is thus exactly propagated (to the accuracy of the perturbation model and integration algorithm). The second-order approximation only affects the representation of the indirect random contributions of the rate functions $R(\xi_N)$ and $D(\xi_N)$ and will only impact the accuracy of the statistical properties of the orbital state (mean and variance). The Jacobian matrix includes the linear component of the indirect random contribution. It will refine the propagation of the state variance. The Hessian matrix introduces the nonlinear component (to second-order) of the indirect random contribution. It will cause the mean trajectory of the satellite to deviate from its deterministic trajectory. These remarks will soon be confirmed in the analytics and the simulations. The first-order Taylor expansion can easily be generated from Eq. (26) by setting $\Delta^2 R_N$ to zero. When ΔR_N is also set to zero, we obtain the zeroth-order Taylor expansion where only the direct random contribution is modeled.

Propagation Equations for the Mean and Variance

When we substitute the stochastic expansion (26) into the augmented set of state difference equations

$$\xi_{N+1} = \xi_N + R(\xi_N) + D(\xi_N)\Gamma_N \tag{27a}$$

$$\Gamma_{N+1} = a\Gamma_N + bW_N \tag{27b}$$

and neglect random deviations δ_N of third and higher order, we get

$$\xi_{N+1} = A_N \xi_N + H_N + \Delta^2 R_N \delta_N \delta_N^T + D_N \Gamma_N + \Delta D_N \delta_N \Gamma_N \tag{28}$$

where

$$A_N \triangleq 1 + \Delta R_N, \qquad 1 = \text{unit matrix } (5 \times 5) \tag{29}$$

$$H_N \triangleq R_N - \Delta R_N \mu_N$$

From this result can be derived the second-order propagation equations for the mean μ_N, random deviation $\delta_N = \xi_N - \mu_N$, and variance σ_N^2 of the orbital state

$$\mu_{N+1} = \mu_N + R_N + \Delta^2 R_N \sigma_N^2 + \Delta D_N \sigma_{\xi\Gamma N}^2 \tag{30a}$$

$$\delta_{N+1} = A_N \delta_N + \Delta^2 R_N (\delta_N \delta_N^T - \sigma_N^2) + D_N \Gamma_N + \Delta D_N (\delta_N \Gamma_N - \sigma_{\xi\Gamma N}^2) \tag{30b}$$

$$\sigma_{N+1}^2 = A_N \sigma_N^2 A_N^T + D_N \sigma_\Gamma^2 D_N^T + A_N \sigma_{\xi\Gamma N}^2 D_N^T + D_N \sigma_{\Gamma\xi N}^2 A_N^T \tag{30c}$$

It can also be shown[7] that the cross-covariance matrix $\sigma_{\Gamma\xi N}^2$ is propagated with

$$\sigma_{\xi\Gamma N+1}^2 = (\sigma_{\Gamma\xi N+1}^2)^T = a[A_N \sigma_{\xi\Gamma N}^2 + D_N \sigma_\Gamma^2] \tag{30d}$$

In the first-order approximation (linearization of the indirect random contribution), these equations degenerate to

$$\mu_{N+1} = \mu_N + R_N \qquad \text{(deterministic case)} \tag{31a}$$

$$\delta_{N+1} = A_N \delta_N + D_N \Gamma_N \tag{31b}$$

$$\sigma_{N+1}^2 = A_N \sigma_N^2 A_N^T + D_N \sigma_\Gamma^2 D_N^T + A_N \sigma_{\xi\Gamma N}^2 D_N^T + D_N \sigma_{\Gamma\xi N}^2 A_N^T \tag{31c}$$

$$\sigma_{\xi\Gamma N+1}^2 = (\sigma_{\Gamma\xi N+1}^2)^T = a[A_N \sigma_{\xi\Gamma N}^2 + D_N \sigma_\Gamma^2] \tag{31d}$$

In the zeroth-order case (direct contribution only), they are

$$\mu_{N+1} = \mu_N + R_N \qquad \text{(deterministic case)} \tag{32a}$$

$$\delta_{N+1} = \delta_N + D_N \Gamma_N \tag{32b}$$

$$\sigma_{N+1}^2 = \sigma_N^2 + D_N \sigma_\Gamma^2 D_N^T + \sigma_{\xi\Gamma N}^2 D_N^T + D_N \sigma_{\Gamma\xi N}^2 \tag{32c}$$

$$\sigma_{\xi\Gamma N+1}^2 = (\sigma_{\Gamma\xi N+1}^2)^T = a[\sigma_{\xi\Gamma N}^2 + D_N \sigma_\Gamma^2] \tag{32d}$$

Comments on the Propagation of the Mean

By examining Eqs. (31a) and (32a) for the first- or zeroth-order stochastic expansions, one observes that the propagation of the mean state μ_N coincides with that for the deterministic state. This conclusion is explained by the fact that a linear Taylor expansion in the random deviations removes all the stochastic effects on a mean trajectory driven by a stationary random process. When the second-order nonlinear terms are added, as shown in Eq. (30a), the mean trajectory starts to deviate from the deterministic one, even though the driving random process has a zero mean. This difference is simply an illustration of the fact that the mean of a nonlinear function is not identical to the nonlinear function of the mean. This effect will be observed in the simulation results.

Comments on the Propagation of the Variance

Unlike the mean, examination of Eqs. (30c), (31c), and (32c) reveals that the propagation of the variance differs for stochastic expansions of order zero and one, but is the same for order one and two. In the zeroth-order case, only the direct contribution of drag (σ_Γ) affects the state variance. This is mathematically demonstrated by suddenly switching off this contribution, i.e., by letting $\sigma_\Gamma^2 = \sigma_{\xi\Gamma}^2 = 0$ in Eq. (32c). At that time, the variance starts to propagate according to

$$\sigma_{N+1}^2 = \sigma_N^2 \tag{33}$$

which effectively means that the variance is no longer affected. For the first- and second-order approximations, the evolution of the variance is additionally affected by the *indirect* contributions of the random rates caused by the random state. The nature of this effect depends on the stability of the matrix A_N.

To illustrate this point, we again turn off the direct contributions in Eq. (30c) and (31c) to obtain the following propagation equation:

$$\sigma^2_{N+1} = A_N \sigma^2_N A^T_N \tag{34}$$

Clearly, σ^2_N will be amplified or attenuated depending on whether the eigenvalues of A_N are outside or inside the unit circle. Because of the definition of A_N [Eq. (29)], this condition reflects on the sign of the first-order derivatives in ΔR_N. The dominant first-order derivatives (drag perturbation with respect to altitude) are *positive*, since the drag perturbation is negative and tends to zero as the altitude increases. Hence, from Eq. (34) one can expect the variance of the orbital state to grow with time, even when the direct random contribution is switched off. In some cases, however, *negative* first-order derivatives may dominate, and a decrease in the variance may result. For instance, the perigee height (above the flattened Earth) is a sinusoidal function of the argument of perigee, and an alternation of positive and negative first-order derivatives will result. This modulation of the variance by the indirect contributions will also be illustrated in the numerical results.

The following table summarizes the particularities of each order of expansion.

Partial Derivatives

Our earlier requirement to derive an analytical solution to the orbital averages becomes justified by the need to evaluate the Jacobian and Hessian matrices associated with the orbital equations. The development of these first- and second-order partial derivatives is described in Ref. 7. Some general comments are provided below.

Since there are three orbital elements (ω, Ω, t) that are driven by the J_2 gravity perturbation (see Appendix), which itself depends on two variables (a, e), there are six first-order and nine second-order partial derivatives associated with gravity. For drag, there are four first-order partial derivatives (a and e are driven by functions of a and e) and, because of their negligible magnitude, the second-order ones are neglected. The drag partial derivatives are evaluated in three steps. First, the derivatives of the LEM with respect to the free parameters ρ_p, σ_0, and σ_1 (and with respect to the orbital elements appearing explicitly in the LEM) must be evaluated. This tedious analytical exercise is somewhat alleviated by the nice properties of the two-dimensional hyperbolic Bessel functions expressed in Eq. (18). Next, the mathematical relations between these free parameters and the GEM must be differentiated. Finally, the partial derivatives of the GEM with respect to the orbital elements must be evaluated. This last task has also been simplified with the use of an exponential form for the global model[7] (GEM).

Results

The propagation equations have been implemented in a multiorbit integration algorithm where the variable step size is an integral multiple of the orbital period. Among the various options offered to the user by the software is the possibility to select the order of stochastic expansion (0, 1, or 2). In this way, one can easily observe the relative magnitude of the direct and indirect random contributions and the effects of the linear and nonlinear stochastic terms.

For illustration, a nearly circular ($e = 0.01$), inclined ($i = 40$ deg) orbit with a perigee height of 300 km is propagated for periods of up to 1020 orbits, i.e., about two months. To represent typical random density variations in the simulations, the following values for the correlation time constant $1/\beta$ and the standard deviation σ_Γ, taken from Ref. 11, have been assumed:

$$1/\beta = 6.2 \text{ days}, \qquad \sigma_\Gamma = 0.20$$

These values represent the statistics associated with the solar activity variations, i.e., $(F_{10.7} - \bar{F}_{10.7})$. When they are combined with Eqs. (23) and (24), the filter parameters can be computed:

$$a = 0.99, \qquad b = 0.028$$

Although the time variation of the modulation factor $M(z_p, t_p)$, shown in Eq. (10), could be taken into account in the simulation, the following constant values for M_1 and M_0 (derived from Ref. 11) were assumed for simplicity:

$$M_1 = 0.01, \qquad M_0 = -0.81$$

The mean and variance of all five orbital elements (a, e, ω, Ω, t) were propagated. In addition, the altitude of the perigee z_p above the flattened figure of the Earth is also monitored. In order to avoid an excessive number of graphs, only the perigee height z_p and the argument of perigee ω are illustrated. This selection is now explained.

The perigee height z_p is strongly influenced by air drag and will demonstrate the direct random contribution of the density variations. The perigee height is also the only variable, in the present model, that can have an alternation of positive and negative first-order derivatives. In fact, as the line of apsides rotates under the J_2 influence, the perigee height increases or decreases depending on whether the perigee is moving toward the flattened pole or the bulging equator of the Earth. As predicted in the equations of motion, these sign changes will cause an alternation of amplifications and attenuations in the variance. This will be observed in the numerical results.

The three variables perturbed by gravity (ω, Ω, and t) are affected by the indirect contribution alone, and they all have a similar statistical evolution. For this reason, and also because of its close relationship with z_p, only the argument of perigee ω is illustrated in the graphical results.

Propagation of the Variance

The time history of the variance in z_p is observed in Fig. 1a, where σ_{z_p} is plotted over 500 orbits (about one month) for stochastic expansions of order 0, 1, and 2. The monotonic growth in the zeroth-order standard deviation (solid curve) only contains the direct contribution of Γ_N. For stochastic expansions of order 1 and 2, which are coincident according to Eqs. (30c) and (31c), the predicted oscillatory effects of the indirect contribution is observed (dashed line). The first- and second-order variances of orbital elements a and e (not shown) do not have such an oscillatory evolution (no sign change in the first-order derivatives) and show a monotonic increase which is larger than that of their zeroth-order one.[7] Figure 1b shows the evolution of the standard deviation of ω (σ_ω). As expected, there is no direct effect on the variance since, in the present model, the argument of perigee is not directly perturbed by air drag. Accordingly, we have $\sigma_\omega \equiv 0$ for order 0. However, since the J_2 perturbation on ω depends on the random position of the satellite, the rate functions indirectly contribute to the increase in the variance of ω. This is illustrated in Fig. 1b (dashed line) for expansions of order 1 and 2. Similar results[7] (not shown) are observed for orbital elements Ω and t.

Propagation of the Mean

The mean trajectory of variables z_p and ω is shown in Fig. 2, again for stochastic approximations of order 0, 1, and 2. In Fig. 2a, the initial increase in perigee height is caused by the initial increase in ω, which moves the perigee away from the equatorial plane of the Earth. As expected from Eqs. (31a) and (32a), the mean trajectory corresponding to orders 0 and 1 coincides with the deterministic propagation of the orbit. For the second-order approximation, the dashed line shows the departure of the trajectory from the deterministic one. This deviation is caused by the nonlinear stochastic terms. As explained earlier, even though the orbital dynamics are driven by a zero-mean random process, their nonlinear characteristics transform the probability distribution function of the orbital

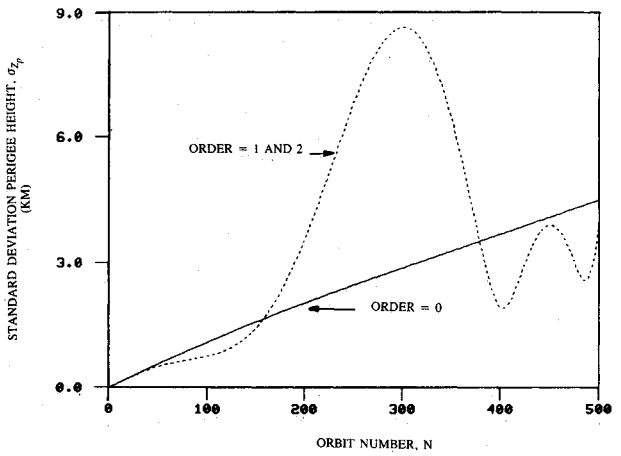

Fig. 1a Standard deviation of the perigee height.

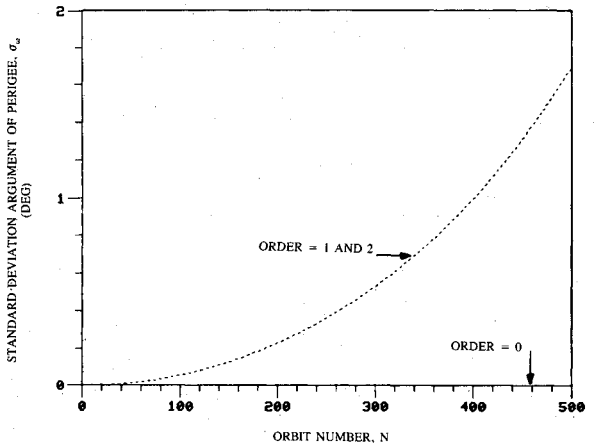

FIg. 1b Standard deviation of the argument of perigee.

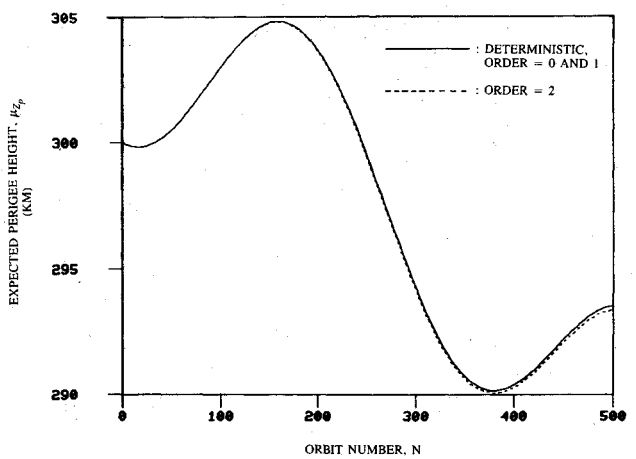

Fig. 2a Mean perigee height.

state such that the mean trajectory no longer corresponds to the deterministic orbital evolution. To be able to observe the same nonlinear effect on ω, it is necessary to propagate it for over two months (1020 orbits), as seen on Fig. 2b. Because this orbital element is only *indirectly* affected by the random perturbations, the nonlinear influence is predictably quite small.

Uncertainty Envelope

Finally, Fig. 3 illustrates the mean (μ) and $\mu \pm \sigma$ trajectories of the perigee altitude over about one month. It can be observed that the 2σ uncertainty grows to about 8 km within this relatively short period.

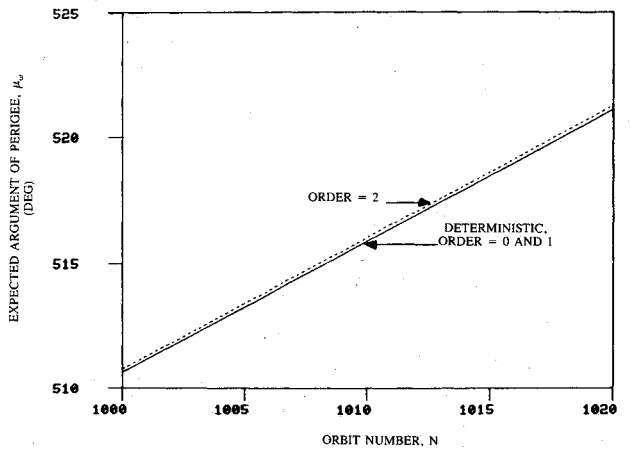

Fig. 2b Mean argument of perigee.

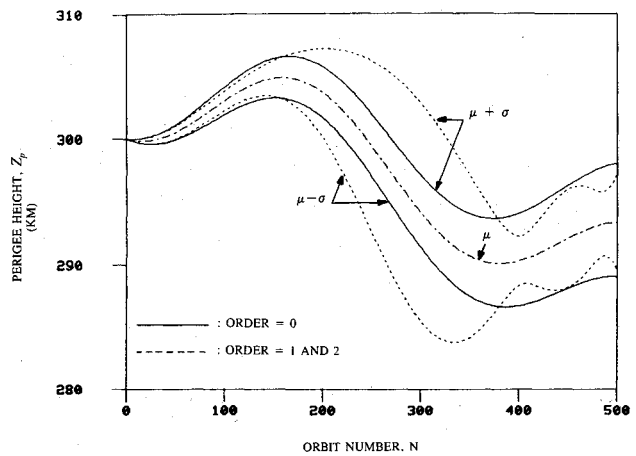

Fig. 3 Uncertainty envelope ($\pm 1\ \sigma$) of the perigee height.

Conclusions

This paper has presented an algorithm for the prediction and dispersion analysis of a low-Earth orbit affected by geopotential oblateness and random drag perturbations. The deterministic part of the motion equations is obtained from a semi-analytic transformation of the variation-of-parameter equations using the method of averaging. The full nonlinearity of the original equations of deterministic motion is kept in the formulation; no further approximations (e.g., linearization) restrict the propagation of the state to small displacement from a reference state.

The stochastic part of the algorithm results from a second-order stochastic Taylor expansion in powers of zero-mean random variables. This technique allows the modeling of both the direct random contribution of the atmospheric density and the so-called indirect contribution that arises from the dependence of the orbital rates on the random position of the satellite. It is shown analytically that the stochastic expansion to zeroth and first order yields mean trajectories that coincide with the deterministic one. The second-order expansion introduces nonlinear terms that induce a deviation of the mean trajectory from the deterministic one. Under a zeroth-order expansion, the variance of the state steadily increases under the effect of the direct random contribution. When the expansion is increased to the first and second order, this monotonic growth in the variance is further modulated by the indirect contribution. The nature and importance of this modulation depends on the sign of the associated first-order derivatives of the orbital accelerations.

Based on this algorithm, a software has been developed to conduct simulations with stochastic expansion of order 0 (di-

rect contribution only), order 1 (direct and linearized indirect contributions), and order 2 (direct and nonlinear indirect contributions). The numerical simulation of a 300-km-high near-circular orbit driven by typical random density variations has confirmed the conclusions obtained from analysis. It also shows that the uncertainty in the orbit size and shape (a and e) grows quite rapidly, whereas that in the other orbital elements (orbital plane orientation) builds up more slowly.

In addition to providing a tool for sensitivity analyses, orbit determination, and atmospheric density estimation, this algorithm has contributed new results in the analytical averaging of the drag perturbation. A more accurate exponential density model has been developed by making its scale-height parameter a function of altitude. The associated drag averages have been expanded in a series of newly defined analytical functions whose properties greatly simplify the development of the partial derivatives required in the stochastic expansion.

Appendix

After analytical averaging of the equations of motion, the following expressions describing the per-orbit changes in the orbital elements are obtained[7]:

$$\frac{da}{dN} = -2\pi B a^2 \rho_p \exp(x_0)\left\{\frac{1}{2}\left[(1+e^2)\hat{X}_0 + 2e\hat{X}_0^c\right]L_0(x_1,x_2) + \sum_{m=1}^{\mathcal{L}a}\left[(1+e^2)\hat{X}_m + 2e\hat{X}_m^c\right]L_m(x_1,x_2)\right\}$$

$$\frac{de}{dN} = -2\pi B a(1-e^2)\rho_p \exp(x_0)\left\{\frac{1}{2}\left[e\hat{X}_0 + \hat{X}_0^c\right]L_0(x_1,x_2) + \sum_{m=1}^{\mathcal{L}e}\left[e\hat{X}_m + \hat{X}_m^c\right]L_m(x_1,x_2)\right\}$$

$$\frac{d\omega}{dN} = \frac{3}{2}\pi J_2\left(\frac{r_E}{p}\right)^2(4 - 5\sin^2 i)$$

$$\frac{di}{dN} = 0$$

$$\frac{d\Omega}{dN} = -3\pi J_2\left(\frac{r_E}{p}\right)^2\cos i$$

$$\frac{dt}{dN} = \Upsilon_0\left[1 - J_2\left(\frac{r_E}{p}\right)^2\left(1 - \frac{3}{2}\sin^2 i\right)(1-e^2)^{1/2}\right]$$

where Υ_0 is the unperturbed orbital period, $B = C_D A/m$ the ballistic parameter of the satellite, $p = a(1-e^2)$ the semilatus rectum, and N the orbit number. The terms in the square brackets of the expressions for a and e depend uniquely on the eccentricity e, and their detailed structure can be found in Ref. 7.

Acknowledgments

This work was supported by the Natural Science and Engineering Research Council of Canada through a Science Scholarship. The author is grateful to the Department of Communications (Government of Canada), which provided the computing facilities necessary for the simulations. The author also wishes to thank Professor P. C. Hughes of the University of Toronto for his technical support during the conduct of this study.

References

[1]McNish, A. G., and Lincoln, J. V., "Prediction of Sunspot Numbers," *EOS Transactions,* Aug. 1949, p. 673.

[2]Holland, R. L., and Vaughan, W. W., "Lagrangian Least-Squares Prediction of Solar Flux ($\bar{F}_{10.7}$)," *Journal of Geophysical Research,* Vol. 89, No. A1, 1984.

[3]King-Hele, D. G., *Theory of Satellite Orbits in an Atmosphere,* Butterworths, London, 1964, pp. 11-16.

[4]King-Hele, D. G., "Methods for Predicting Satellite Orbital Lifetimes," *Journal of the British Interplanetary Society,* Vol. 31, No. 5, 1978, p. 181.

[5]Liu, J. J. F., France, R. G., and Wackernagel, H. B., "An Analysis of the Use of Empirical Atmospheric Density Models in Orbital Mechanics," Space Command, Peterson Air Force Base, CO, Spacetrack Rept. 4, 1983.

[6]Elyasberg, P. E., Kugaenko, B. V., Synitsyn, V. W., and Voiskovsky, M. I., "Upper Atmosphere Density Determination from the COSMOS Satellite Deceleration Results," Akademie-Verlag, Berlin, Space Research XII, 1972.

[7]de Lafontaine, J., "Orbital Dynamics in a Stochastic Atmosphere and a Nonspherical Gravity Field," Ph.D. Dissertation, Univ. of Toronto Inst. for Aerospace Studies, Rept. 313, 1986.

[8]Liu, J. J. F., "Orbital Decay and Lifetime Estimation," Northrop Services, Inc., Huntsville, AL, TN-240-1441, April 1975.

[9]Alford, R. L., and Liu, J. J., "The Orbital Decay and Lifetime (LIFTIM) Prediction Program," Northrop Services, Inc., Huntsville, AL, Rept. M-240-1278, May 1974.

[10]de Lafontaine, J., and Mamen, R., "Orbit Lifetime Prediction and Safety Considerations," *Space Safety and Rescue 1984-1985,* Paper IAA-84-269; edited by G. W. Heath, AAS Science and Technology Series, Vol. 64, Univelt, San Diego, CA, 1986, pp. 17-60.

[11]Elyasberg, P. E., and Kugaenko, B. V., *Effect of Upper Atmospheric Density Variations on Artificial Earth Satellite Orbits,* Akademie-Verlag, Berlin, Space Research XVI, 1976, p. 175.

[12]Rauch, H. E., "Optimum Estimation of Satellite Trajectories Including Random Fluctuations in Drag," *AIAA Journal,* Vol. 3, No. 4, 1965, p. 717.

[13]Meyer, P. L., "Introductory Probability and Statistical Applications," Addison-Wesley, Reading, MA, 1970.

[14]de Lafontaine, J., and Garg, S. C., "A Review of Satellite Lifetime and Orbit Decay Prediction," *Proceedings of the Indian Academy of Sciences (Engineering Sciences),* edited by S. Ramaseshan, Vol. 5, Indian Academy of Sciences, Bangalore, India, Sept. 1982; pp. 197-258; also, Univ. of Toronto Inst. for Aerospace Studies, Toronto, Canada, UTIAS Review 43, Dec. 1979.

[15]Jacchia, L. G., "Thermospheric Temperature, Density and Composition: New Models," Smithsonian Astrophysical Observatory, Special Rept. 375, March 1977.

[16]de Lafontaine, J., and Hughes, P. C., "A Semianalytic Satellite Theory for Orbital Decay Predictions," *Journal of the Astronautical Sciences,* Vol. 35, No. 3, 1987, pp. 245-286.

[17]Cook, G. E., and King-Hele, D. G., "The Contraction of Satellite Orbits Under the Influence of Air Drag. V: With Day-to-Night Variation in Air Density," *Philosophical Transactions of the Royal Society,* Vol. 259A, 1965, pp. 33-67.

[18]Chen, S. C. H., "Ephemeris Generation for Earth Satellites Considering Earth Oblateness and Atmospheric Drag," Northrop Services, Inc., Huntsville, AL, Rept. M-240-1239, May 1974.

[19]Santora, F. A., "Satellite Drag Perturbations in an Oblate Diurnal Atmosphere," *AIAA Journal,* Vol. 13, No. 9, 1975, p. 1212.

[20]Watson, J. S., Mistretta, G. D., and Bonavito, N. L., "An Analytic Method to Account for Drag in the Vinti Satellite Theory," *Celestial Mechanics,* Vol. 11, 1975, pp. 145-177.

[21]Willey, R. E., and Pisacane, V. L., "The Motion of an Artificial Satellite in a Nonspherical Gravitational Field and an Atmosphere with a Quadratic Scale Height," *Journal of the Astronautical Sciences,* Vol. 21, No. 5-6, 1974, p. 230.

[22]Morrison, J. A., "Generalized Method of Averaging and the Von Zeipel Method," *Methods in Astrodynamics and Celestial Mechanics,* edited by R. L. Duncombe and V. G. Szebehely, Academic, New York, 1966.

[23]Kyner, W. T., "Averaging Methods in Celestial Mechanics," *The Theory of Orbits in the Solar System and in Stellar Systems,* edited by G. Contopoulous, Academic, New York, 1966.

[24]Liu, J. J. F., "A Second-Order Theory of an Artificial Satellite Under the Influence of the Oblateness of the Earth," AIAA Paper 74-166, Jan.-Feb. 1974.

[25]Liu, J. J. F., and Alford, R. L., "A Semi-Analytic Theory for the Motion of a Close-Earth Artificial Satellite with Drag," AIAA Paper 79-0123, Jan. 1979.

[26]Cefola, P. J., Long, A. C., and Holloway, J., Jr., "The Long-Term Prediction of Artificial Satellite Orbits," AIAA Paper 74-170, Jan.-Feb. 1974.

[27]Green, A. J., and Cefola, P. J., "Fourier Series Formulation of the Short-Periodic Variations in Terms of Equinoctial Variables," AIAA Paper 79-133, June 1979.

[28]de Lafontaine, J., "The Derivation of a Second-Order Satellite

Trajectory Predictor in Terms of Geometrical Variables," *Acta Astronautica,* Vol. 13, No. 8, 1986, pp. 481-489.

[29]Liu, J. J. F., and Alford, R. L., "Transformations and Variational Equations for an Artificial Satellite About an Oblate Earth—Part 1," Northrop Services, Inc., Huntsville, AL, TN-240-1199, Feb. 1973.

[30]Cefola, P. J., and McClain, W. D., "A Recursive Formulation of the Short-Periodic Perturbations in Equinoctial Variables," AIAA Paper 78-1383, Aug. 1978.

[31]McClain, W. D., Long, A. C., and Early, L. W., "Development and Evaluation of a Hybrid Averaged Orbit Generator," AIAA Paper 78-1382, Aug. 1978.

[32]Fuchs, A. J., Diamante, J. M., Dunn, P. J., and Torrence, M., "Rapid Satellite Lifetime Estimation," Goddard Space Flight Center, Systems Development and Analysis Branch, Greenbelt, MD, Aug. 1975.

[33]Broucke, R. A., and Cefola, P. J., "On the Equinoctial Orbital Elements," *Celestial Mechanics,* Vol. 5, No. 3, 1972, pp. 303-310.